

# Experimental and numerical investigation of flow structure and heat transfer during high pressure condensation in a declined pipe at COSMEA facility

Thomas Geißler<sup>a,\*</sup>, Rita Szijarto<sup>b</sup>, Matthias Beyer<sup>a</sup>, Uwe Hampel<sup>a,c</sup>, H.-M. Prasser<sup>b</sup>, S. Leyer<sup>d</sup> and M. Walther<sup>e</sup>

<sup>a</sup>Helmholtz Zentrum Dresden Rossendorf, Institute of Fluid Dynamics, Experimental Thermal Fluid Dynamics, Bautzner Landstraße 400, 01328 Dresden, Germany

<sup>b</sup>Paul Scherrer Institut, Laboratory for Thermal Hydraulics, 5232 Villingen, Switzerland

<sup>c</sup>Technische Universität Dresden, Institute of Power Engineering, AREVA Endowed Chair of Imaging Techniques in Energy and Process Engineering, 01062 Dresden, Germany

<sup>d</sup>Université du Luxembourg, Faculty of Science, Technology and Communication, Campus Kirchberg, 6, rue Coudenhove-Kalergi, L-1359 Luxembourg

<sup>e</sup>AREVA GmbH, Paul-Gossenstr. 100, 91052 Erlangen, Germany

---

## Abstract

Reliability and safety are perpetual topics in the development of nuclear installations. Generation III reactor concepts contain additional passive safety systems for improved accident control and mitigation. Main aspect of these passive systems is to operate with a minimum of external energy and signals. One example is the emergency condenser of the KERENA reactor concept, which removes heat from the core passively, e.g. after a station blackout. The governing natural circulation flow with condensation is only coarsely understood and current simulation methods need to be improved. During the condensation process a complex interaction between flow structure and heat transfer takes place and this determines the total efficiency of the passive safety system and hence the reliability in managing an incident.

The experimental facility COSMEA (condensation test rig for flow morphology and heat transfer studies) at HZDR is designed to provide experimental results to support the further development of CFD calculation methods. The test rig consists of a 3 m long emergency condenser pipe (ID 43 mm) which is 0.76° inclined and cooled by forced water flow. The experiments are conducted in a pressure range between 5 bar and 65 bar with steam mass flow rates up to 1 kg/s. Measurements of pressure, temperature, flow rate and condensation rate deliver integral understanding of the process. To investigate the details of the resulting stratified flow structures, x-ray tomography is applied. Parallel temperature measurements inside the heat transferring wall provide information about the azimuthal distribution of the heat flux.

A phase injection system was developed to operate the experiment in a stepwise condensation mode, which allows the measuring of condensation rates, flow morphologies and heat transfer distribution for different steam fraction values. The combination between cross sectional images from x-ray tomography and the azimuthally resolved heat transfer clarify the coupling between flow structure and heat transfer during condensation.

The experimental results are supported by a system code calculation. The COSMEA facility was modeled with the RELAP5 code. The original condensation model of the code was modified such that the heat transfer coefficient depends on the local mass fraction of the flow field. The experimental and calculation results agreed well for the steady state condensation process in the condensation rate, secondary side temperature and the heat flux data.

## 1 Introduction

Currently constructed nuclear power plants meet safety requirements mostly relying on active safety systems. However, advanced nuclear power plant designs utilize passive safety systems achieving better safety. Passive safety systems operate without external power supply or operator intervention, only relying on physical laws, as natural circulation and gravity driven flows (International Atomic Energy Agency, 2009).

The KERENA™ boiling water reactor, developed by AREVA, acquires the advantages of a Gen-III+ nuclear reactor design, as it is economically efficient due to the simple operational and configuration design and the passive safety control (Stosic et al., 2008). It features a two-stage passive heat transfer system for core decay heat removal (Figure 1). The reactor concept contains several passive safety systems such as passive pulse transmitter (actuator), core flooding lines, drywell flooding lines, pressure suppression and venting systems for pressure reduction and hydrogen blow off, emergency condenser and containment cooling condenser. Additional large water volumes (core flooding pool, pressure suppression pool, shielding pool) are provided.

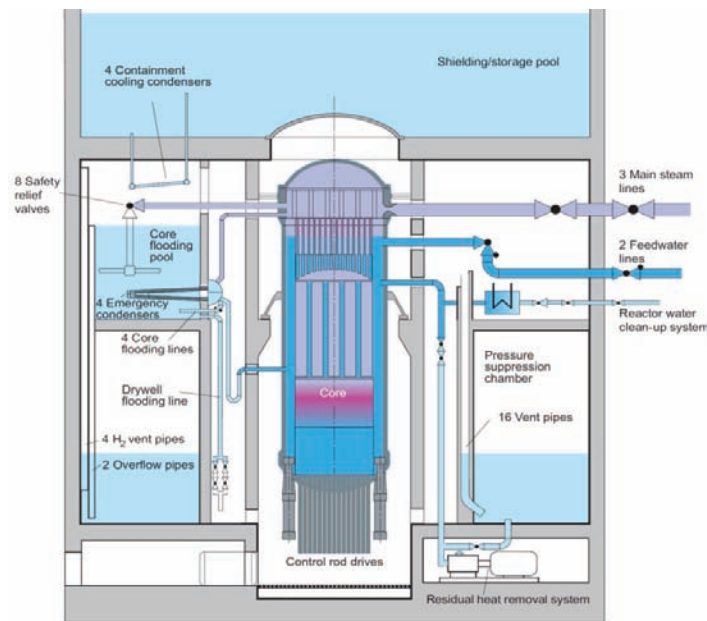


Figure 1: Overview over safety features of the KERENA reactor concept (taken from Stosic et al., 2008).

The passive pulse transmitter is a passive switching device. The switching function is done by a pilot operated valve. The valve is opened by a confined liquid that is in thermal connection to a stand pipe of the pressure vessel. In an accident scenario, the liquid is heated, and due to the expansion, the valve is actuated. Several flooding lines feed the reactor core and the drywell with cold water from elevated water storage tanks. These large water volumes around the pressure vessel also used as a condensation trap for vented steam.

The core decay heat in an accident scenario is removed from the reactor pressure vessel in two steps (Wagner et al., 2011). The emergency core cooling system is connected to the reactor pressure vessel at two locations. Should the water level drop in the reactor pressure vessel, steam enters the horizontal condensation pipes and condensates on the pipe walls. The pipes are located in the core flooding pool; thus, the heat is transferred to the containment. The heat is removed from the containment by a containment cooling system, which is connected to a large water pool outside the containment and thus to the environment. To lower the pressure during this cooling procedure, steam is blown and thus condensed into the water filled pressure suppression chamber. Therefore the operation of the emergency cooling change takes place in a transient pressure mode.

The present work aimed at analysing the flow morphology in the emergency core cooling system of the KERENA reactor. The emergency condenser consists of slightly inclined horizontal pipes, which are connected to the secondary side. Condensation occurs on the colder pipe walls, and the condensate film flows in axial

direction, driven by the interfacial shear, and along the pipe wall towards the bottom due to gravity, forming a stratified flow pattern (Palen et al., 1979). Consequently, the liquid film is asymmetric to the azimuthal coordinate. A wavy gas-liquid interface is expected due to the high shear induced by the steam flow. The stratified height increases along the axial coordinate, and isolated bubbles are produced by the larger waves, forming a slug or plug flow. These flow patterns have a significant influence on the heat transfer (El Hajal et al., 2003). Both the turbulent inner convection in the liquid phase as well as the highly agitated interface makes it impossible to derive a simple heat transfer coefficient for the film and rivulet from first principles.

For the KERENA emergency condenser, integral thermal hydraulic tests have been performed at the INKA test facility at AREVA in Karlstein (Leyer and Wich, 2012). The INKA experiments provided boundary conditions for the COSMEA experiment series, which is introduced in this paper. The NOKO facility at the Research Centre Jülich was constructed to investigate the effectiveness of the emergency condenser (Li et al., 2001; Prasser et al., 1997; Schaffrath et al., 1999). Based on these experiments, the ATHLET extension KONWAR for condensation heat transfer in declined pipes was developed (Schaffrath, 1997). In related experiments at the TOPFLOW facility at Forschungszentrum Dresden-Rossendorf, the single phase convection and particularly problems of thermal stratification on the secondary (pool) side of a horizontal heat exchanger were experimentally studied and simulated with state-of-the-art CFD methods (Krepper and Beyer, 2010). The present study aimed at continuing the analysis of the emergency core cooling system, providing high-resolution data for local flow regime and heat transfer in a horizontal pipe. The COSMEA facility is dedicated to the detailed analysis of flow and condensation heat transfer on the primary high-pressure side of the cooling system, i.e. inside the heat exchanger tubes. The experiments were made with a dense instrumentation and provide thermal hydraulic data for further model development.

In the nuclear industry, one-dimensional system codes are prevailing to simulate entire nuclear power plants, and to analyze the reliability of the safety systems. The RELAP5 code, developed by the US. NRC, was used to calculate the measurement matrix of the COSMEA facility. The original condensation model for horizontal pipes was replaced by a model, which considers the local flow pattern in the pipe cross section through the mass fraction and the stratification angle (Szijártó et al., 2014). The calculations showed very good agreement with the experimental data.

## 2 Experimental setup and instrumentation

### 2.1 Experimental Facility

The COSMEA facility (condensation test rig for flow morphology and heat transfer studies, Figure 2) consists of an annular pipe system, with the inner pipe resembling a section of the emergency condenser. The condensation pipe is made of stainless steel with an inner diameter of 43.3 mm and a wall thickness of 2.5 mm. The length of the cooled section is 3225 mm. The condensation pipe is jacketed by a 120 mm titanium pipe, which ensures the cooling of the pipe by a forced counter-current flow to allow well-defined cooling conditions (small temperature increase, 3K or 5K; cooling water temperature during the experiment  $T_{in}=40^{\circ}\text{C}$ ). During the measurements, the cooling water is circulated with high volume flow in an internal circuit driven by a pump. Additionally 5 swirl generators were inserted into the annular gap. The first one near the cooling water inlet and the following near the 4 temperature measurement positions along the test section (see Figure 3). To keep the averaged cooling water temperature on an almost constant level in spite of the different test conditions (cooling power), a specified amount of “fresh” cooling water is fed into the internal cooling circuit by a second pump via the cooling water fed line and the same mass flow of heated cooling water is drained in the TOPFLOW blow off tank. The pressure in the internal cooling circuit can be set in a range of 2 to 5 bar. The chosen operating regime should simulate the heat removal in large water pool by providing a constant cooling water temperature, nevertheless is the heat transfer of a forced convective flow slightly higher, than for pool circulation (Fuhrmann, 1985, p. 25).

At the inlet of the inner pipe a mixing device for steam and saturated water is installed. The supply of steam and saturated water is maintained by the TOPFLOW (Prasser et al., 2006) steam circuit. The typical operating conditions of this configuration are depicted in Table 1. This permits starting conditions for the condensation process with a wide variety of inlet conditions.

The mixing device consist of a ring injection system which generates an annular flow morphology by tangentially inject a liquid water ring around a steam core flow. Due to swirling effects caused by the tangential injection of the liquid a flow straightener is inserted into the central tube short after the inlet injector. After the mixing unit the fluid flows into the inner tube of the test section. At the initial section the condensation tube is insulated against cooling water. This thermal insulation part of the tube can be considered as adiabatic flow inlet length that finally results to more than 10 L/D.

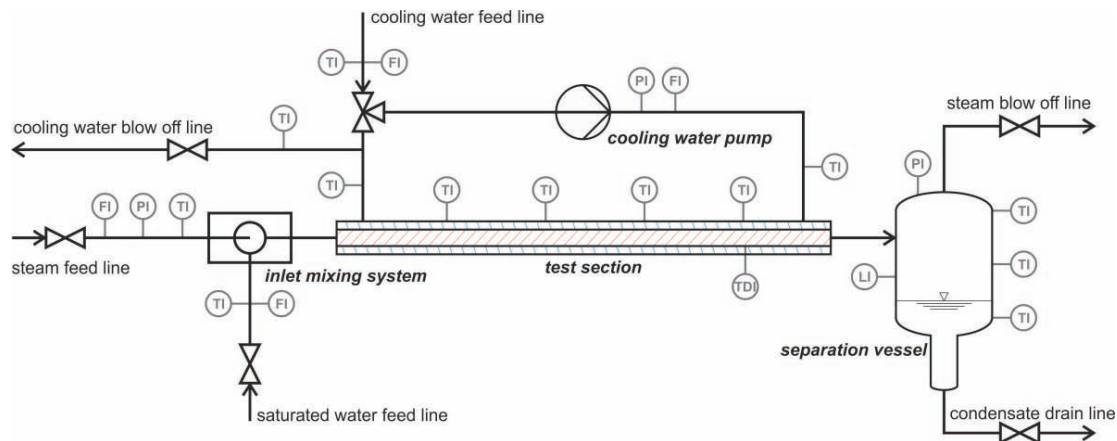


Figure 2: Flow scheme of the COSMEA facility with the test section including the connections to the TOPFLOW facility and the instrumentation.

The condensation pipe terminates into a separation vessel, which is a vertical pressure vessel with an inner diameter of the upper part of 550 mm and of the bottom part of 177 mm. This design allows the determination of the condensation rate in a wide range (50g/s ... 300g/s) by measuring the level increase gradient in the tank. The test section is connected tangentially to the upper part of the separation tank so that the two-phase flow separates inside the tank due to centrifugal forces. The liquid drains through the condensate drain line into the blow-off tank of the TOPFLOW facility.

The experimental set-up is equipped with an x-ray tomograph and a heat flux probe to study flow morphology and heat transfer during condensation respectively. The central condensation pipe (grey) and the measurement planes for temperature measurement and tomography are depicted in Figure 3. X-ray tomography opens the possibility to obtain cross-sectional images of the local flow morphology without intrusion. On the basis of these data the flow pattern and fluid distribution inside the condensation pipe can be disclosed. The heat flux probe contains thermocouples equally distributed in azimuthal position inside the wall of the condensation pipe to derive the local heat flux at one axial position.

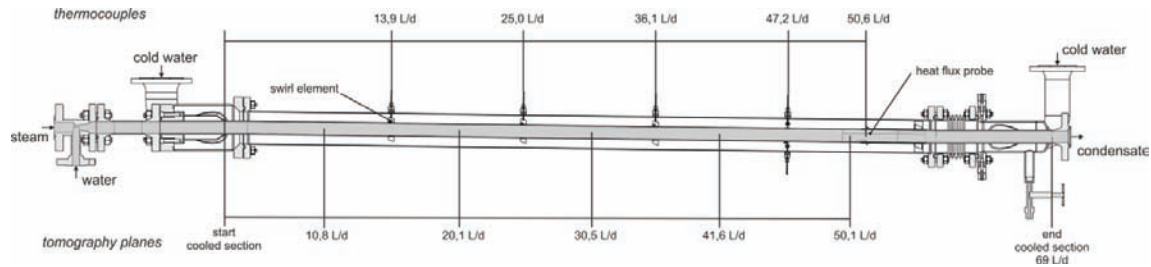


Figure 3: Sectional view of the test section. Position of temperature measurements and tomography planes in dimensionless length.

Beside the instrumentation along the heat exchanger section the experiment is equipped with variety of other measurement devices. These are pressure transducers at the mixture inlet after the ring injector, in the separation vessel and inside the cooling water. The steam and saturated water mass flow is measured by four Coriolis mass flow meters and the cooling water circulation and feed water are measured with vortex flow meters. Additionally the cooling water is equipped with thermocouples at the entrance and outlet of every loop.

## 2.2 Experimental procedure

At the beginning of each experimental campaign steam from the steam generator flows into the air filled condensation tube and separation tank to heat it up. The steam mass flow is adjusted in such a way that during the heat-up procedure steam always reaches the separation tank, independent of the condensation rate in the test section. Thereby the water drainage valve blows off the mixture of condensate and air. This procedure leads to an optimal degassing of the test rig. During the heat-up procedure of the primary side, the pressure and the temperature level of the secondary side is controlled and adjusted to the required values. When all boundary conditions are satisfied, the X-ray tomograph starts to measure the flow regime inside the condensation tube. During steady-state operation five cross-sectional images are captured over the length. After the X-ray scan completes, the liquid blow-off valves close and the level increase due to the accumulation of the condensate in the separator vessel is recorded.

Table 1: Range of experimental parameters of the condensation experiments at the TOPFLOW facility.

<i>steam parameters</i>		<i>pressure - mass flow parameters</i>	
pressure	5 - 65 bar	5 bar	0.088 kg/s
temperature	151 – 286 °C	15 bar	0.314 kg/s
steam mass flow	0.088 – 0.8 kg/s	25 bar	0.406 kg/s
water mass flow	0 – 0.555 kg/s	45 bar	0.610 kg/s
		65 bar	0.800 kg/s
<i>cooling water parameters</i>			
pressure	3.5 -4.5 bar		
water mass flow	15 - 30 kg/s		
temperature	40 °C		
<i>test section parameters</i>			
length	3.3 m	material	1.4571 (stainless steel)
inclination	0.76 °		
inner diameter	43.3 mm	Number of experiments	23

The COSMEA facility is adapted to the needs of the measurement techniques. This contains the use of a forced convection cooling for easy accessibility, an outer titanium pipe to reduce x-ray attenuation by auxiliary constructional parts and the scaling of the length of the condensation pipe. Especially the length scaling leads to a lower heat transfer capability in comparison the reference INKA experiments. During one steady state experiment only a part of the injected steam can be condensed, so the whole condensation range is splitted into up to six single experiments starting with the outlet conditions of the previous run as inlet condition.

Therefore the experimental series at 65 bar condensation pressure, for example, is divided in six consecutive experiments. This approach delivers data at various steam fractions along the condensation progress.

Based on experimental data gained in the large scale tests at the INKA facility the mass flow rate at the different pressure levels is fixed. All of the presented results refer to the individual mass flow shown in Table 1.

The process control system is coupled with a data acquisition server to store operational data with a frequency of 1Hz. Measurements of the heat flux probe are taken separately with a temporal resolution of 3Hz. Both acquisition systems are triggered by the start of the x-ray tomograph to ensure simultaneous values.

### 2.3 Wall heat flux measurement

The heat flux probe measures the temperature along the heat transfer path through the tube wall. The heat flux is determined with a measured wall thickness and the material properties by help of the Fourier law (equation 1). The wall heat flux is calculated for five different azimuthal positions (index k) with the temperature difference between primary and secondary side of the wall ( $T_{prim}-T_{sec}$ ), the thermal conductivity of the used stainless steel at mean temperature and the measured thickness of the tube wall  $d_k$ .

$$\dot{q}_{wall,k} = \lambda(\bar{T}) \frac{(T_{prim} - T_{sec})_k}{d_k} \quad k = \{0^\circ, 45^\circ, 90^\circ, 135^\circ, 180^\circ\} \quad 1$$

To measure wall temperatures at the inner and outer wall of the stainless steel pipe 0.5 mm type K class 1 thermocouples are used. The thermocouples pairs are welded into the surfaces of the tube at primary and secondary sides at five angular positions. The thermocouple configuration of the heat flux probe is shown in Figure 4.

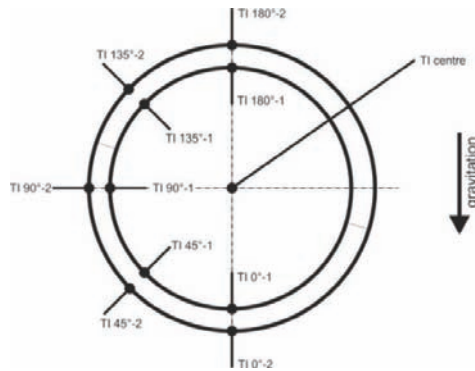


Figure 4: Sketch of the position and nomenclature of each thermocouple inside the heat flux probe.

### 2.4 X-ray tomography measurement

As it is mentioned in section 2.1, the experimental setup is equipped with an x-ray tomograph on a horizontal positioning unit. The tomography system consists of a beam source which is represented by a medical x-ray tube (Varian medical systems, RAD 56) with characteristic operation parameters of acceleration voltage of 130 kV and anode current of 13 mA / 16 mA. The detector is a flat panel x-ray detector (1024x1024 pixel, Perkin Elmer RID 1640) in opposition to the x-ray tube. Both components are mounted on a frame which can be turned 210 ° around the double tube test section. During one rotation of the frame 240 radioscopic images are collected within 3 min 30 s. The data of this stack of radioscopic images is used to recalculate a cross sectional image of the object by filtered back projection. This approach leads to a time averaged cross sectional image of the flow structure inside the condensation pipe. Fast fluctuations, interfacial waves or slugs cannot be resolved. The resulting grey value images are used to determine the height of the water flow at the ground of the tube (rivulet height called in the following). The detection of the transition between the two phases is done by a threshold method for every image. The threshold value is defined for each image as the average grey value between pure steam in the core section and pure condensate at the bottom of the rivulet.

### 3 Experimental results

#### 3.1 Condensation rate

One significant property of the condensation process is the condensation rate. The present work determines the amount of condensate per time by three independent methods. The level rise method is already mentioned in section 2.2 and is based on the level / volume slope inside the separation vessel. To get the correlation between hydrostatic pressure (level) and volume a calibration of the vessel volume is done. The second and third calculation methods are based on the cooling water energy balance. The secondary side balance takes into account the heat up of the cooling water mass flow countercurrent to the condensation section. A second energy balance, the feed water balance, is based on the amount of cooling water which needs to be replaced with cold water to maintain the cooling water temperature constant.

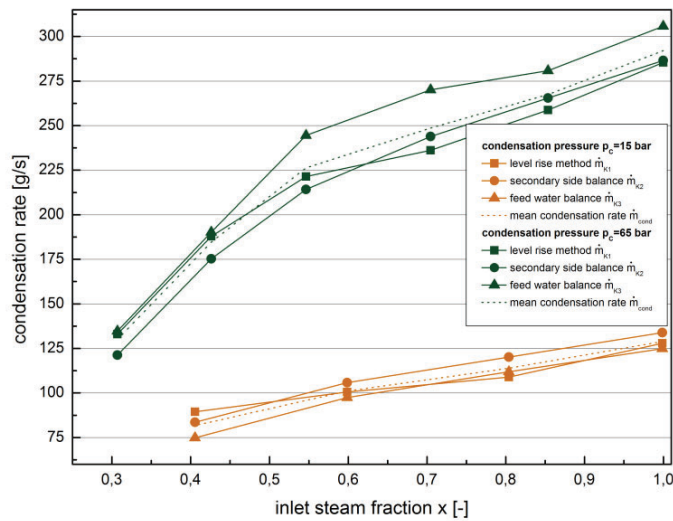


Figure 5: Comparison of the condensation rate over steam fraction at 15 bar and 65 bar for three independent methods ( $\dot{m}_{15\text{bar}}=0.256$  kg/s,  $\dot{m}_{65\text{bar}}=0.8$  kg/s ).

Figure 5 compares the mentioned calculation methods for experiments at 15 bar and 65 bar. It can be shown, that all of the three methods fit together with a maximum deviation of 15%. An influence of the inlet steam fraction is not recognisable. An averaged condensation rate is calculated by weighting the different approaches on the basis of their measurement uncertainty.

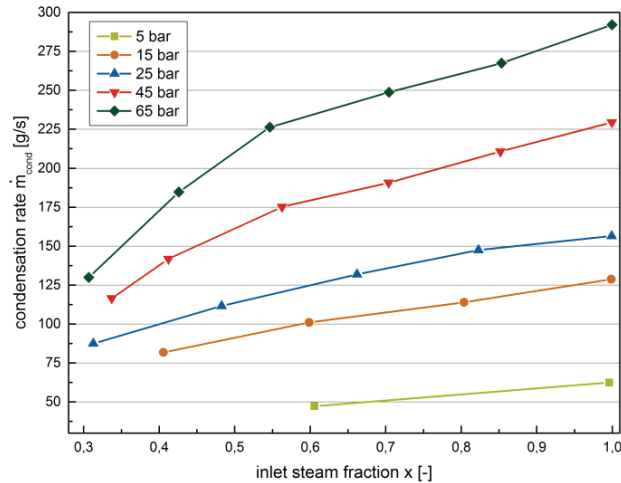


Figure 6: Averaged condensation rate for experiments between 5 bar and 65 bar for different inlet steam fractions

Figure 6 shows the averaged condensation rate for the done 23 experiments at five different pressure levels against the inlet steam fraction. The highest condensation rates are achieved at a pressure of 65 bar and the lowest with experiments at 5 bar. This trend corresponds with the decrease in saturation temperature respective temperature difference toward the heat sink. For a condensation process starting at steam  $x=1$  at the inlet the condensation rate differs between 0.292 kg/s and 0.062 kg/s. The condensation rates decrease by decreasing the inlet steam fraction. At 65 bar a decrease by 55% is observed. With lower pressure this effect gets less. The mentioned behavior can be explained by the increase of liquid mass fraction and thus increase of the rivulet height and the reduction of effective heat transfer area.

### 3.2 Wall heat flux

Figure 7 shows the measured angular resolved heat flux for experiments at 15 bar and consecutive inlet steam fractions. The heat flux reaches the highest values with pure steam at the inlet with 700 kW/m<sup>2</sup>. By increasing the condensate content the local heat transfer decreases at all azimuthal positions. It can be found that the measurement positions at the bottom of the tube is strongest influenced from the increasing liquid mass flow. This effect is extended to the 45° position at inlet steam fraction of  $x=0.4$ . The described effect is explained by the heat transfer mechanism during film condensation. An existing water film on the heat transfer surface is the major heat transfer resistance. By decreasing the steam fraction, the liquid water film is increasing. Due to the near horizontal orientation of the test section a stratified flow is established and hinders the heat transfer at the lowest measurement positions inside the tube. This assumption is proofed by tomographic measurements at experimental conditions (see 3.3).

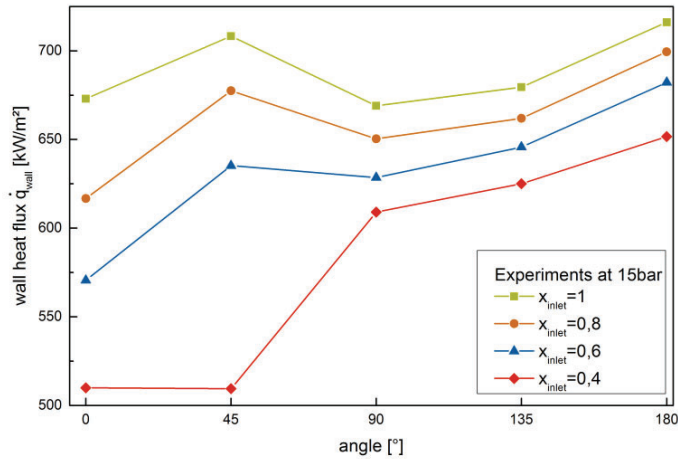


Figure 7: Wall heat flux at different angular positions at 15 bar with different inlet steam fractions.

To get information about the entire condensation process out of the consecutive experiment the angular resolved measurements of the heat transfer are averaged regarding the corresponding heat transfer area of their measurement positions. By assuming a constant heat flux over the pipe length during one single experiment, the inlet steam fraction, the geometric position of the heat flux probe and the determined condensation rate a virtual steam fraction at the heat flux probe position is assessable. The resulting heat flux over the steam fraction at the done pressure levels is given in Figure 8. The heat flux level can clearly be distinguished between the individual pressure levels. The highest values are achieved for 65 bar experiments and the lowest at 5 bar. In general there is a trend to lower heat fluxes at lower steam fractions caused by the above described phenomena. The slope of the shown curve is larger at higher pressure because of the increased injected total mass flow and therefore the possibility to occupy a larger surface area with a thick water film.

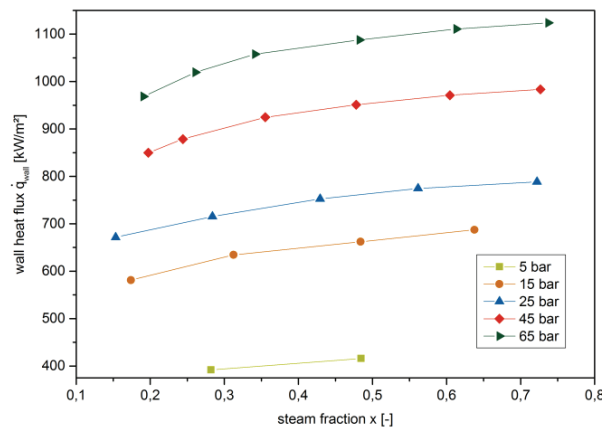


Figure 8: Area averaged wall heat flux at different pressure over a wide range of the condensation process.

### 3.3 Flow morphology

Following the assumptions made in the previous paragraphs there is the necessity to have a simultaneous consideration of heat transfer effects and the corresponding flow structure. Figure 9 gives the determined height of the rivulet flow for six consecutive experiments each with five measurement positions over the length at 65 bar. By assuming a constant condensation rate for one steady state experiment and the geometrical relations an assignment toward a steam fraction is done. The chart illustrates the overlapping of the single consecutive runs and depicts the reached reproducibility (within 2 mm) of the measurement principle. In general rivulet height grows by decreasing steam fraction up to 13.5 mm at  $x=0.2$ .

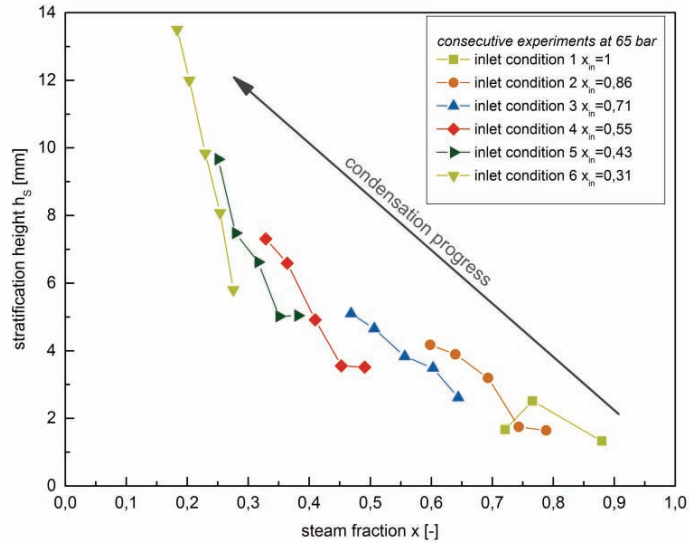


Figure 9: Rivulet height at 65 bar experiments with changing condensation progress from six consecutive experiments.

On the basis of the previous findings the determined rivulet height for all 23 experiments are plotted over the calculated steam fraction in Figure 10. The general trend of an increasing water level height with decreasing steam fraction is clearly observed. Furthermore is there no clear distinction between the pressure levels regarding the connection of stratification and steam fraction. A possible explanation is the origin of the experimental parameters. Each pressure level is investigated at a certain total mass flow which was chosen after integral test with a natural circulation loop in a large scale facility (Leyer and Wich, 2012). In natural circulation phenomena exists a connection between mass flow and driving forces. That means for the present case, that the driving force is simulated by a forced flow at a certain predefined pressure dependent mass flow. The acceleration of the liquid phase in stratified flow is mainly caused by shear interactions with the flowing gas phase. The height of the water level is the result of the force balance between gas and liquid phases. In the present case the changes in properties due to the different pressure are compensated by the change in mass flow. Therefore there is no distinction of the rivulet height against the pressure levels.

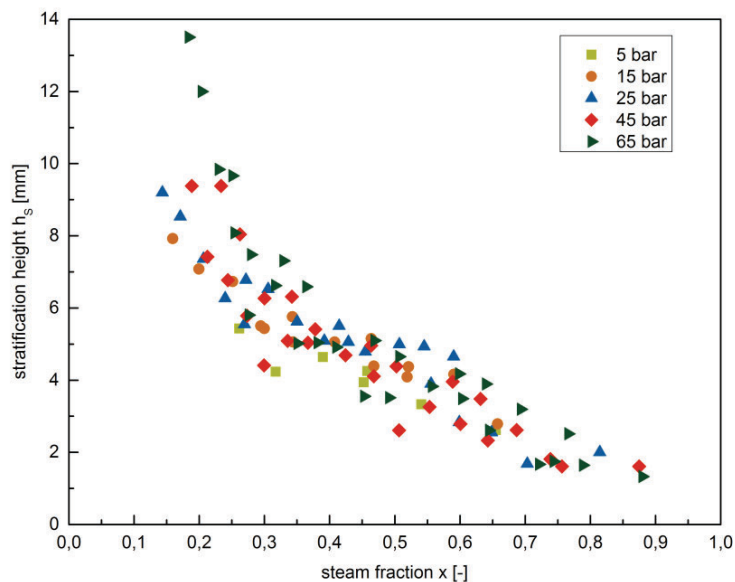


Figure 10: Rivulet height at different pressure.

#### 4 One-dimensional simulations with RELAP5

The COSMEA facility was modeled with the RELAP5 code. The original condensation model of the code was modified (Szijártó et al., 2014) such, that the heat transfer coefficient depends on the local mass fraction of the flow field. The heat transfer area is divided into two parts. At the upper peripheral part laminar film condensation is assumed, and in the bottom part axial turbulent flow and single phase heat transfer is considered. The stratification angle effect is taken into account, which plays an important role during the condensation process.

The model of the COSMEA setup consisted of two pipes, which were connected by a heat structure (Figure 11). The heat structure is a 2.5 mm wall, modeled as stainless steel. The condensation pipe was connected to an adiabatic inlet and outlet pipes. The inlet conditions were set by two time dependent junctions, which ensured the correct mass fraction and mass flow for the steam-water mixture. A third time dependent junction was connected to the secondary side inlet.

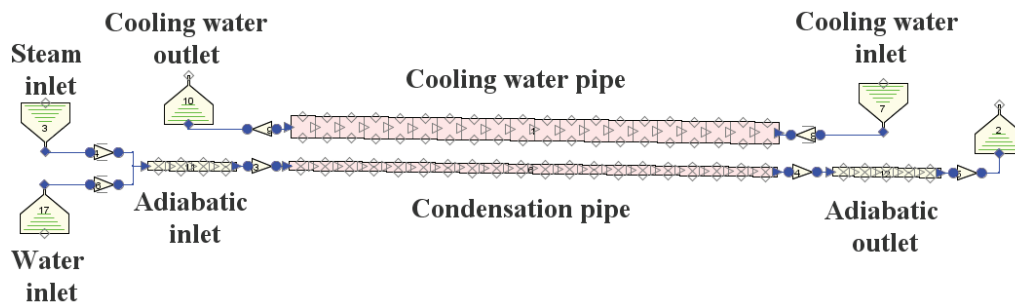


Figure 11: Nodalisation scheme of the COSMEA experiment.

All the 23 initial conditions were used to calculate the condensation process. The RELAP5 code was run in a transient mode, until the steady state condition was reached. The steady state conditions were compared to the experimental data.

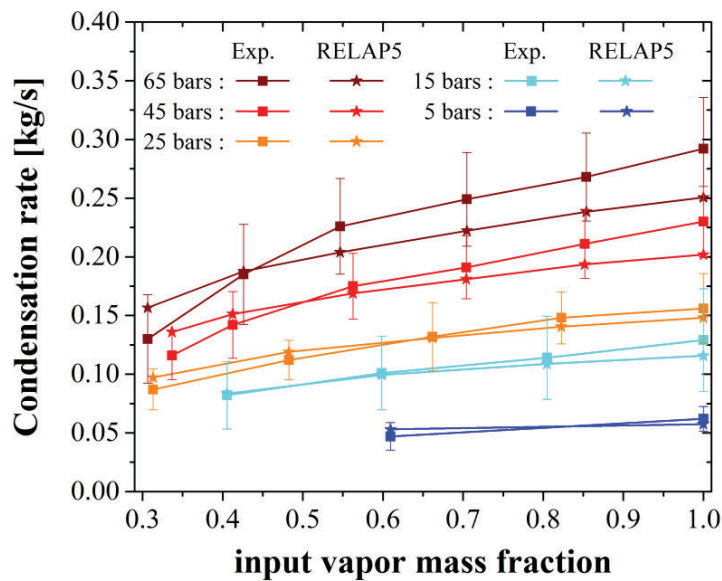


Figure 12: Comparison between measured and calculated condensation rates.

Figure 12 shows the comparison for the measured and simulated condensation rates for all the experiments. The condensation rate was an output of the RELAP5 calculation for all the nodes. The condensation rate was summed for the adiabatic inlet, outlet and the condensation pipe separately. The inlet part had a condensation mass flow about 0.5%, because of the initial subcooling of the water and steam. The outlet adiabatic section had a contribution of about 7-10% to the final condensation rate, due to the subcooling of the water.

The sum of the three parts was compared to the experimental results. The two data fitted for all the experimental results within the error limit. The comparison resulted in a higher difference for the high and low mass fraction experiments. The highest difference, for the experiment 65-6, was 20%. Apart from the lowest and highest initial mass fractions, the difference between the calculated and measures condensation rate values was in a range of 1--10%.

Figure 13 shows the comparison for the heat flux data. The heat flux was taken from the RELAP5 output for the node at the same location as the heat flux probe in the experiment. The experimental heat flux was the average of the five heat flux probe values. The results fitted well, the highest difference was for the low mass fraction and low pressure experiments (5-1 - 21%, 5-2 - 20%, 15-3 - 15%, 15-4 - 26%, 25-5- 22%, 45-6 - 12%, 65-6 - 10%). For all the other experiments the difference between the experimental results and the simulated results was lower than 8%.

The temperature of the secondary side was measured at 6 positions in the experiment, at the inlet, the outlet, and 4 positions along the condensation section. The error of thermocouples was 0.3 K. The azimuthal and radial temperature distribution showed that the swirl generators ensured the homogeneous temperature field in the pipe within 1.5 K.

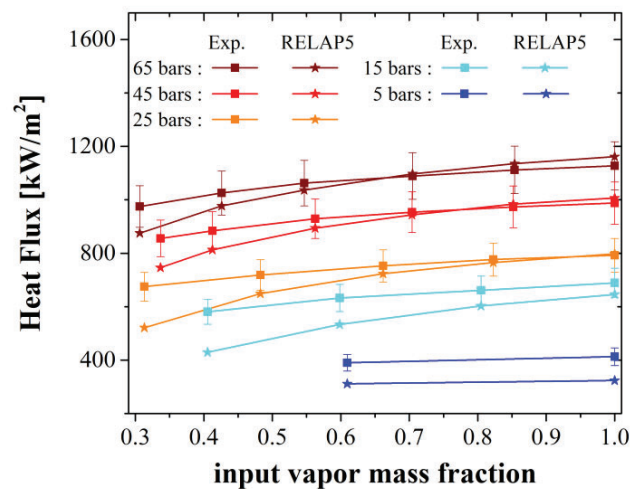


Figure 13: Comparison between measured and calculated heat flux.

Table 2 shows the comparison of the secondary side temperature. The inlet temperature was set corresponding to the experimental inlet conditions. Therefore, the outlet temperature data, and the temperature difference were compared. The two data sets fitted in the error limit.

Table 2: Comparison of the measured and calculated secondary side temperatures.

No.	$T_{Outlet}(R5)$ [K]	$T_{Outlet}(Exp.)$ [K]	$\Delta T (R5)$ [K]	$\Delta T (Exp)$ [K]	$ \Delta T (R5) - \Delta T (Exp) $ [K]
5-1	313.555	313.85	1.905	2.2	0.295
5-2	313.606	313.85	1.956	2.2	0.244
15-1	313.774	314.05	1.924	2.2	0.276

No.	$T_{Outlet}(R5)$ [K]	$T_{Outlet}(Exp.)$ [K]	$\Delta T (R5)$ [K]	$\Delta T (Exp)$ [K]	$ \Delta T (R5) - \Delta T (Exp) $ [K]
15-2	313.616	313.85	1.966	2.2	0.234
15-3	313.568	313.85	1.918	2.2	0.282
15-4	313.563	313.95	1.813	2.2	0.387
25-1	314.28	314.45	3.630	3.8	0.170
25-2	314.328	314.35	3.578	3.6	0.022
25-3	314.321	314.45	3.671	3.8	0.129
25-4	314.313	314.45	3.663	3.8	0.137
25-5	314.032	314.45	3.382	3.8	0.418
45-1	314.999	315.15	3.449	3.6	0.151
45-2	314.142	314.15	3.592	3.6	0.008
45-3	314.245	314.25	3.595	3.6	0.005
45-4	314.263	314.35	3.613	3.7	0.087
45-5	313.888	313.95	3.638	3.7	0.062
45-6	314.175	314.25	3.625	3.7	0.075
65-1	316.046	316.35	3.396	3.7	0.304
65-2	315.520	315.75	3.470	3.7	0.230
65-3	316.597	316.85	3.447	3.7	0.253
65-4	316.388	316.65	3.438	3.7	0.262
65-5	316.203	316.45	3.453	3.7	0.247
65-6	316.118	316.35	3.468	3.7	0.232

The experimental and calculation results agreed well for the steady state condensation process in the condensation rate, secondary side temperature and the heat flux data.

## 5 Conclusion

The COSMEA condensation experiments in a single effect test rig at pressures between 5 bar and 65 bar expand the knowledge about flow structure and heat transfer during the operation of a passively driven heat removal system. The experiments complement the large scale tests of the AREVA INKA facility to bridge from laboratory scale experiment to real scale power plant application. The experiments had been done at a novel test setup with extensive measurement equipment to obtain experimental data with a high resolution. Special attention was paid to investigate wall temperatures and the flow morphology during the condensation process. Main results are azimuthal wall temperatures and the resulting heat flux of the condensation process, condensation rates at different steam fractions and the characterisation of the existing flow during the condensation process over a wide steam fraction range. The obtained measurement data is used as a reference for a new RELAP 5 model to describe condensation phenomena. The simulations show a good agreement to the measured values.

## Acknowledgment

This work was supported by the financial support and the industrial knowledge of the AREVA GmbH in the frame of a collaborative research project.

## Nomenclature

RPV	Reactor pressure vessel
$\dot{m}$	Mass flow rate [kg/s]
x	Steam mass fraction [kg/kg]
COSMEA	Condensation test rig for flow morphology and heat transfer studies

## References

- El Hajal, J., Thome, J., Cavallini, A., 2003. Condensation in horizontal tubes, part 1: two-phase flow pattern map. *Int. J. Heat Mass Transf.* 46, 3349–3363.
- Fuhrmann, H., 1985. *Verfahrenstechnische Berechnungsmethoden 1*. Deutscher Verlag für Grundstoffindustrie, Leipzig.
- International Atomic Energy Agency, 2009. *Passive safety systems and natural circulation in water cooled nuclear power plants - IAEA TECDOC 1624*. International Atomic Energy Agency, Vienna, Austria.
- Krepper, E., Beyer, M., 2010. Experimental and numerical investigations of natural circulation phenomena in passive safety systems for decay heat removal in large pools. *Nucl. Eng. Des.* 240, 3170–3177.
- Leyer, S., Wich, M., 2012. The Integral Test Facility Karlstein. *Sci. Technol. Nucl. Install.* 2012, 1–12.
- Li, W., Hicken, E., David, P.H., Prasser, H.-M., Baldauf, D., Zschau, J., 2001. Messung der Kondensatfilmthicken in einem dampfdurchstroemten horizontalen Rohr. Presented at the Annual meeting on nuclear technology 2001, Dresden.
- Palen, J.W., Breber, G., Taborek, J., 1979. Prediction of Flow Regimes in Horizontal Tube-Side Condensation. *Heat Transf. Eng.* 1, 47–57.
- Prasser, H.-M., Beyer, M., Carl, H., Manera, A., Pietruske, H., Schütz, P., Weiß, F.-P., 2006. The multipurpose thermalhydraulic test facility TOPFLOW : an overview on experimental capabilities, instrumentation and results. *Kerntechnik* 163–173.
- Prasser, H.-M., Böttger, A., Schaffrath, A., 1997. Strömungsformen bei Kondensationsvorgängen im Notkondensator-Versuchsstand, FZR-186. Forschungszentrum Rossendorf.
- Schaffrath, A., 1997. KONWAR - eine Erweiterung von ATHLET zur Berechnung der Kondensation in waagerechten Rohren ( No. 3343), Berichte des Forschungszentrums Jülich. Forschungszentrums Jülich, Jülich.
- Schaffrath, A., Prasser, H.-M., Hicken, E., Jaegers, H., 1999. Experimental and analytical Investigation of the operation mode of the emergency condenser of the SWR1000. *Nucl. Technol.* 2, 123–142.
- Stosic, Z.V., Brettschuh, W., Stoll, U., 2008. Boiling water reactor with innovative safety concept: The Generation III+ SWR-1000. *Nucl. Eng. Des.* 238, 1863–1901.
- Szijártó, R., Freixa, J., Prasser, H.-M., 2014. Simulation of condensation in a closed, slightly inclined horizontal pipe with a modified RELAP5 code. *Nucl. Eng. Des.* 273, 288–297.
- Wagner, T., Wich, M., Doll, M., Leyer, S., 2011. Full Scale Tests with the Passive Core Flooding System and the Emergency Condenser at the Integral Test Stand Karlstein for KERENA. In: *Proceedings of ICAPP'12*. Presented at the ICAPP 2011, Nice.